

1
2
3
4
5
6
7
8
9
10
11
12
13
14
15
16
17
18
19
20
21

An *in situ* high-pressure NMR study of sodium coordination
environment compressibility in albite glass

Sarah J. Gaudio^{1*}, Trenton G. Edwards², Sabyasachi Sen²

¹Department of Earth and Planetary Sciences, University of California, Davis, California 95616,
USA

²Division of Materials Science and Engineering, University of California, Davis, California,
95616, USA

*Corresponding author (e-mail sjgaudio@ucdavis.edu)

REVISION 1

22

Abstract

23 The pressure dependent modification of the Na-O coordination environment in albite
24 glass is studied *in situ* to 2 GPa using high-pressure solid-state ^{23}Na nuclear magnetic resonance
25 spectroscopy. Compression of the glass at ambient temperature results in shortening of the Na-O
26 bond distance. The concomitant decrease in volume of the local Na-O coordination environment
27 alone can account for the bulk compressibility of albite glass at 300 K. These results provide the
28 first direct experimental evidence of a collapse of the open aluminosilicate framework that helps
29 explain previously reported densification of aluminosilicate glasses and liquids at relatively low
30 pressures without accompanying change in the average coordination number of the network
31 forming Al and Si cations. Such structural changes at relatively low pressures may have far
32 reaching implications for the mechanistic understanding of compressibility and viscosity
33 anomalies characteristic of open tetrahedral aluminosilicate network glasses and melts of
34 geological importance.

35

36 *Keywords: in situ, high pressure, NMR, glass structure, compressibility, albite, sodium aluminosilicate*

37

38

Introduction

39 The physical properties of vitreous and molten $\text{NaAlSi}_3\text{O}_8$ (hereafter referred to as albite)
40 have been studied extensively as an analog for strongly polymerized melts generated and
41 differentiated in the Earth's crust. Although the thermal expansion, compressibility, and
42 viscosity of albite glass/liquid at 1 atm conditions are relatively well constrained (e.g. Kress et al.
43 1988; Lange 1996; Sipp et al. 2001), one must extrapolate these physical properties to higher
44 pressures to model the magmatic processes that occur within the Earth. Accurate predictions of

45 silicate melt properties at pressure depend on detailed understanding of the structural changes
46 accompanying their densification.

47 Albite, like silica, is a fully connected three-dimensional network of corner-shared
48 $[\text{AlO}_{4/2}]^{-1}$ and $[\text{SiO}_{4/2}]^0$ tetrahedra. Much like silica, but with $(\text{Na}^+ + \text{Al}^{3+})$ substituted for 1/4 of
49 the Si^{4+} , albite glass at 1 atm maintains an open framework structure. Na^+ cations occupy the
50 large holes within the aluminosilicate framework and charge-compensate for the negatively
51 charged $[\text{AlO}_{4/2}]^{-1}$ tetrahedra (Lee and Stebbins 1999, 2000). Both albite and silica glass are
52 highly compressible, and become more compressible with increasing pressure below ~ 2.5 GPa
53 (Bridgeman et al. 1925; Kuryaeva and Surkov 2010; Sonnevile et al. 2013). This behavior is
54 considered to be anomalous as it is the opposite of what is expected and observed for crystals
55 with the same chemistry (Benusa et al. 2005).

56 While the changes in the density of albite and silica glass are large within the first few
57 GPa of compression, the concomitant structural changes of the coordination environments of the
58 network forming cations are found to be rather subtle. X-ray diffraction (XRD) studies of albite
59 glass structure recovered from pressures <2.0 GPa identify only minor distortions of the
60 tetrahedral network (Hochella and Brown Jr. 1985). On the other hand, samples synthesized at
61 relatively high pressures >6 GPa show shortening of both the Na-O (Lee et al., 2006) and T-O (T
62 = Si,Al) bond distances, reduction of the intertetrahedral bond angles $\langle\text{T-O-T}^\circ\rangle$ (Stebbins and
63 Sykes 1990; Sykes et al. 1993) and the presence of some Al coordinated by >4 oxygens (Yarger
64 et al. 1995; Allwardt et al. 2005). The lack of major changes to glass structure at low pressure
65 forced these studies to speculate that the shortening of the Na-O bond distance must be the
66 dominant mechanism of densification, similar to what is observed in perovskites with organic
67 charge-balancing cations (e.g. Swainson et al. 2007), and indicative of a collapse of the open

68 tetrahedral framework in the region of anomalous compressibility, as mentioned above.
69 However, this hypothesis lacks direct experimental confirmation because such pressure-induced
70 topological changes are either partially or fully reversible on decompression making the
71 evaluation of their true nature and extent impossible for *ex situ* structural studies. Observation of
72 nearest-neighbor structural changes associated with elastic deformation requires application of an
73 element-specific spectroscopic technique such as nuclear magnetic resonance (NMR)
74 spectroscopy. The application of solid-state NMR spectroscopy *in situ* at high pressure is limited
75 owing to the technological challenges associated with designing a high-pressure probe head (1)
76 having suitable non-magnetic materials that can operate up to a few GPa, and (2) provides
77 sufficient sensitivity and sample volume. Recently, we developed a high-pressure NMR probe in
78 our laboratory capable of maintaining hydrostatic pressures up to 2.5 GPa. Here, we report the
79 results of an *in situ* high-pressure (HP) static ^{23}Na NMR spectroscopic study of compression on
80 the Na-O nearest-neighbor coordination environment in albite glass to 2 GPa. We exploit the
81 well-established trends relating the ^{23}Na NMR peak position with the average Na-O distance and
82 coordination number that are reported for sodium aluminosilicate minerals and glasses (Xue and
83 Stebbins 1993; George and Stebbins 1995; Lee and Stebbins 2003) to demonstrate the nature of
84 the pressure-induced elastic deformation of the Na-O coordination environment. This has
85 important implications for understanding the pressure dependence of Na^+ mobility, viscosity, Na
86 partitioning behavior, and the pressure and temperature dependence of bulk albite glass and
87 liquid density.

88

89

Methods

90 The albite glass was prepared at Corning, Inc. in a 5 kg batch from stoichiometric
91 proportions of Puratronic® grade Na₂CO₃, Al₂O₃, and SiO₂ powders. The powder mixture was
92 decarbonated by heating overnight in a box furnace at 873 K and then melted in a platinum
93 crucible at 1873 K for 3 hours. Molten albite was quenched to glass by removing the crucible
94 from the furnace and cooling in air. The recovered glass was crushed and re-melted twice under
95 identical conditions to ensure chemical homogeneity. Electron probe micro-analysis confirmed
96 the homogeneity and near stoichiometric proportions of Na₂O, Al₂O₃, and SiO₂ of the starting
97 glass (Gaudio et al., *In Review*).

98 The *in situ* high-pressure NMR experiments were performed using a custom-built NMR
99 probe where a core-drilled rod of the albite glass (~ 1 mm diameter by 3 mm length) was
100 pressurized using a cylindrical high-pressure cell (*EasyCell 30*, Almax-Easylab) that was
101 configured for NMR measurements (Wang et al. 2011). A simple cross-sectional schematic of
102 the cell configuration is shown in Figure 1. The cell sleeve has an outer and an inner shell made
103 of non-magnetic Cu-Be alloy and MP35N superalloy, respectively (Walker 1999). An NMR coil
104 was wrapped directly onto the sample and the leads were epoxied into a pressure cell feed-
105 through. The sample/coil is fitted inside a Teflon® cylindrical cup filled with Daphne 7373
106 paraffin industrial oil as a pressure transmitting fluid and is held in the pressure sleeve using a
107 locking nut (Otero-Leal et al. 2009). Pressure is applied to the Teflon cup using a hydraulic ram
108 traveling through a hollow locking nut and subsequently advancing a sapphire piston (8mm
109 diameter x 25mm length) from the opposite end of the cell. The piston-side locking nut secures
110 the advancing piston, allowing for the cell to remain pressurized when separated from the
111 hydraulic press. The compression of the Teflon cap and fluid allow for the application of
112 hydrostatic pressure on the sample. Cell pressure was determined from the applied hydraulic

113 pressure that was calibrated in separate runs using the known relationship between pressure and
114 the electrical resistance of a manganin wire (Nomura et al. 1979). The loaded pressure cell is
115 placed in the NMR probe and positioned such that the coil is perpendicular to the applied
116 external magnetic field (additional experimental details are given in Edwards et al. 2014).

117 The ^{23}Na static NMR spectra were collected in a horizontal bore (inner bore diameter of
118 180 mm) 7T Bruker imaging magnet equipped with a BrukerBioSpec spectrometer system
119 operating at a ^{23}Na Larmor frequency of 79 MHz. Single-pulse ^{23}Na NMR spectra were
120 collected at 0.5 GPa intervals in pressure, ranging between ambient (~ 0 GPa) and 2 GPa, using a
121 $\pi/8$ solid pulse (1.5 μs) with a recycle delay of 0.5 s. Approximately 1000 to 2000 free induction
122 decays were averaged and Fourier transformed to obtain each spectrum. Phasing methods and
123 parameters were kept constant for processing of all spectra. Due to the large quadrupolar
124 broadening of the static ^{23}Na line shapes, only relative changes in the spectral peak position as a
125 function of pressure are of interest. Therefore, all ^{23}Na NMR spectra are referenced to the peak
126 maximum of the unpressurized albite glass sample in the pressure cell.

127

128 **Results and Discussion**

129 Static ^{23}Na NMR spectra of albite glass collected *in situ* at pressures from 0 to 2 GPa
130 show a single broad peak with a full width at half maximum of ~ 110 ppm, that does not change
131 significantly with pressure (Fig. 2). Over 2.0 GPa, the frequency of the peak maximum increases
132 by 4.6 ppm relative to the peak maximum position in the non-compressed sample (Fig. 3-top).
133 The relative shift in the ^{23}Na NMR peak position is completely reversible upon decompression,
134 indicating that cold (room temperature) compression on albite glass structure to 2.0 GPa is fully
135 elastic (Fig. 2 and Table 1).

136 Previous work indicates that the Na-O bond distance is inversely proportional to the ^{23}Na
137 isotropic chemical shift (δ_{iso}) for Na sites in crystalline albite (Xue and Stebbins 1993; George
138 and Stebbins 1995). For sodium aluminosilicate glasses and liquids at 1 atm and for those
139 recovered from high pressures, the ^{23}Na NMR spectrum displays a single broad peak (e.g.
140 Oestrike et al. 1988; Maekawa et al. 1997; Lee and Stebbins, 2003; Lee et al. 2006) whose
141 position can be related to the average Na-O bond distance. Systematic studies of aluminosilicate
142 crystals and glass compositions established a relationship of between -0.0155 to -0.0119 Å/ppm
143 (Xue and Stebbins 1993; Angeli et al. 2000; Lee and Stebbins 2003) between the ^{23}Na NMR
144 peak position and the Na-O bond distance. This relationship, in combination with the average
145 Na-O bond distance of 2.71 Å for albite glass prepared at 1 atm (Hochella and Brown Jr. 1985),
146 enables the calculation of the average Na-O bond distance using pressure-dependent relative
147 frequency shift of the ^{23}Na NMR peak maximum obtained in the present study. Substitution of
148 the relative frequency shift of the ^{23}Na NMR peak maximum for the corresponding shift in δ_{iso} is
149 supported by the lack of any significant change in the quadrupolar coupling constant of ^{23}Na
150 nuclides in albite and Na-Ca aluminosilicate glass samples recovered from pressures up to 8 GPa
151 (Lee et al. 2006; Lee 2011). The average Na-O bond distance as a function of pressure is shown
152 in Figure 3(top). The average Na-O distance displays a monotonic decrease with pressure by
153 0.063 ± 0.009 Å or $\sim 2.3\%$ at 2.0 GPa (Fig. 3-top and Table 1). We calculate the decrease in the
154 average volume of the Na-O coordination environment with pressure by assuming the
155 environment is spherical after Wu et al. (2009) using the Na-O bond distance as the sphere's
156 radius (Table 1). Over 2 GPa, the Na-O coordination sphere volume decreases by $6.9 \pm 0.9\%$
157 (Fig. 3-bottom). The changes in volume of the Na-O environment alone and that of bulk albite

158 glass upon compression at ambient temperature (Kuryaeva and Surkov 2010) show remarkable
159 agreement over the same pressure range (Fig. 3-bottom).

160 When taken together, these results directly demonstrate that the majority of the
161 compressibility of the local Na environment accounts for the bulk compressibility of albite glass.
162 It is consistent with the structural scenario for aluminosilicate glasses where the modifier cations
163 occupy the highly compressible “voids” in the open tetrahedral framework. Furthermore, the
164 nearest-neighbor coordination environments of these cations act as a passive indicator of
165 tetrahedral network collapse upon compression at relatively low pressures. In the absence of a
166 significant change in the coordination of the network-forming cations Si^{4+} and Al^{3+} (Gaudio et al.
167 In Review), such network collapse is also likely related to the anomalous compressibility in this
168 low pressure regime that is characteristic of albite and silica glasses with fully polymerized
169 tetrahedral networks (Bridgeman et al. 1925; Kuryaeva and Surkov 2010; Sonnevile et al. 2013)

170

171

Implications

172 The pressure dependence of the ^{23}Na NMR spectra indicates that monotonic reduction of
173 the average Na-O bond length and the corresponding volume reduction of the Na-O nearest
174 neighbor coordination shell accounts for the bulk densification of albite glass to 2 GPa. These
175 results provide confirmation of a long-speculated mechanism of low pressure densification via
176 the collapse of the open tetrahedral aluminosilicate framework, and may have important
177 implications for our mechanistic understanding of the nature of elastic deformation, pressure
178 dependence of element partitioning and viscosity of fully polymerized aluminosilicate magmatic
179 liquids. In particular, volume reduction within the oxygen “cage” for Na^+ should effectively
180 increase its ionic field strength (Angell et al. 1982; Kelsey et al. 2009), a condition that favors

181 the formation of stable high-coordinated Al (Stebbins et al. 2013 and citations therein), which
182 contributes to a decreasing viscosity and increasing density with pressure.

183

184

Acknowledgements

185 This work was supported by a grant from the National Science Foundation (NSF-DMR
186 1104869) to SS.

187

188

Table 1: Pressure, Relative shift of ^{23}Na peak maximum, calculated average Na-O bond distance, Na-O coordination shell volume, and volume change with pressure

Pressure (GPa)	relative shift of peak maximum (ppm)	average Na-O distance** Å	Na-O coordination shell volume Å ³	Relative <i>volume</i> change %
0.0	0	2.710	83.4	0.0
0.5	1.6	2.689±0.003	81.2±0.2	-2.3±0.3
1.0	3.5	2.662±0.006	78.6±0.6	-5.2±0.7
1.5	3.9	2.656±0.007	78.1±0.6	-5.9±0.8
2.0	4.6	2.647±0.009	77.2±0.7	-6.9±0.9
0.0*	0	2.710	83.4	0.0

* Following decompression

**Data from Xue and Stebbins (1993), George and Stebbins (1995), Angeli et al., 2000 and Lee and Stebbins (2003) were used to relate the relative shift of the ^{23}Na peak maximum to the average Na-O distance ($d\langle\text{Na-O}\rangle$) assuming 8 nearest neighbor oxygens. There is some dispersion in the average Na-O versus ^{23}Na chemical shift relationships reported in Lee and Stebbins (2003) and Angeli et al. (2000). Therefore, we report the average of the $d\langle\text{Na-O}\rangle$ bond distance calculated for each relationship, while the uncertainty in this value represents the difference between the average value and the maximum or minimum calculated value. The average_{max} Na-O bond distance is calculated using the Na-O versus ^{23}Na chemical shift relationship given in Lee and Stebbins (2003) where $d\langle\text{Na-O}\rangle = -0.0155 \times (\text{relative shift in peak position}) + 2.71 \text{ \AA}$. The average_{min} Na-O bond distance is calculated using the Na-O versus ^{23}Na chemical shift relationship given in Angeli et al. (2000) where $d\langle\text{Na-O}\rangle = -0.0119 \times (\text{relative shift in peak position}) + 2.71 \text{ \AA}$. 2.71 Å is the average Na-O bond distance in albite glass reported in Hochella and Brown Jr. (1985) and in Xue and Stebbins (1993).

189

References Cited

- 190
191
192 Allwardt, J.R., Poe, B.T., and Stebbins, J.F. (2005) The effect of fictive temperature on Al
193 coordination in high-pressure (10 GPa) sodium aluminosilicate glasses. *American*
194 *Mineralogist* 90, 1453-1457.
195
196 Angeli F., Delaye J.M., Charpentier T., Petit J.C., Ghaleb D. , Faucon P.(2000) Influence of glass
197 chemical composition on the Na-O bond distance: A Na-23 3Q-MAS NMR and molecular
198 dynamics study, *Journal of Non-Crystalline Solids*, 276, 132–144
199
200 Angell, C. A., Cheeseman, P. A., and Tamaddon, S. (1982) Pressure enhancement of ion
201 mobilities in liquid silicates from computer simulation studies to 800 kilobars. *Science* 218,
202 885-887.
203
204 Benusa, M. D., Angel, R. J., Ross, N. L. (2005) Compression of albite, NaAlSi₃O₈. *American*
205 *Mineralogist* 90, 1115-1120.
206
207 Bridgman, P. W. (1925) Compressibility of glasses. *American Journal of Science* 58, 359-367.
208
209 Edwards, T., Endo, T., Walton, J. H., Sen, S. (2014) Observation of the transition state for
210 pressure-induced BO₃→ BO₄ conversion in glass. *Science* 345, 1027-1029.
211
212 George, A. M., and Stebbins, J. F. (1995) High-temperature ²³Na MAS NMR data for albite:
213 Comparison to chemical-shift models. *American Mineralogist* 80, 878-884.
214
215 Hochella, M.F., and Brown, G.E. (1985) The structures of albite and jadeite composition glasses
216 quenched from high pressure. *Geochimica et Cosmochimica Acta* 49, 1137-1142.
217
218 Kress, V. C., Williams, Q., and Carmichael, I. S. (1988) Ultrasonic investigation of melts in the
219 system Na₂O-Al₂O₃-SiO₂. *Geochimica et Cosmochimica Acta* 52, 283-293.
220
221 Kelsey, K.E., Stebbins, J.F., Mosenfelder, J.L., and Asimow, P.D. (2009) Simultaneous
222 aluminum, silicon, and sodium coordination changes in 6 GPa sodium aluminosilicate
223 glasses. *American Mineralogist* 94, 1205-1215.
224
225 Kuryaeva, R. G., and Surkov, N. V. (2010) Behavior of the refractive index and compressibility
226 of albite glass at pressures up to 6.0 GPa. *Geochemistry International* 48, 835-841.
227
228 Lange, R. A. (1996) Temperature independent thermal expansivities of sodium aluminosilicate
229 melts between 713 and 1835 K. *Geochimica et Cosmochimica Acta* 60, 4989-4996.
230
231 Lee, S. K. (2011) Simplicity in melt densification in multicomponent magmatic reservoirs in
232 Earth's interior revealed by multinuclear magnetic resonance. *Proceedings of the National*
233 *Academy of Sciences* 108, 6847-6852.
234

- 235 Lee, S. K., and Stebbins, J. F. (1999) The degree of aluminum avoidance in aluminosilicate
236 glasses. *American Mineralogist* 84, 937-945.
237
- 238 Lee, S. K., and Stebbins, J. F. (2000) The structure of aluminosilicate glasses: high-resolution
239 ^{17}O and ^{27}Al MAS and 3Q MAS NMR study. *The Journal of Physical Chemistry B* 104,
240 4091-4100.
241
- 242 Lee, S.K., and Stebbins, J.F. (2003) The distribution of sodium ions in aluminosilicate glasses: A
243 high-field Na-23 MAS and 3Q MAS NMR study. *Geochimica et Cosmochimica Acta* 67,
244 1699-1709.
245
- 246 Lee, S.K., Cody, G.D., Fei, Y., and Mysen, B.O. (2006) The effect of Na/Si on the structure of
247 sodium silicate and aluminosilicate glasses quenched from melts at high pressure: A multi-
248 nuclear (Al-27, Na-23, O-17) 1D and 2D solid-state NMR study. *Chemical Geology* 229,
249 162-172.
250
- 251 Maekawa, H., Nakao, T., Shimokawa, S., and Yokokawa, T. (1997) Coordination of sodium ions
252 in $\text{NaAlO}_2\text{-SiO}_2$ melts: a high temperature ^{23}Na NMR study. *Physics and chemistry of*
253 *Minerals* 24, 53-65.
254
- 255 Nomura, M., Yamamoto, Y., Ochiai, Y., & Fujiwara, H. (1979) The measurement of the
256 resistance of manganin wire with the cubic-anvil type pressure apparatus. *Japanese Journal*
257 *of Applied Physics* 18, 363-366.
258
- 259 Oestrike, R., Yang, W. H., Kirkpatrick, R. J., Hervig, R. L., Navrotsky, A., and Montez, B.
260 (1987) High-resolution ^{23}Na , ^{27}Al and, ^{29}Si NMR spectroscopy of framework
261 Aluminosilicate glasses. *Geochimica et Cosmochimica Acta* 51, 2199-2209.
262
- 263 Otero-Leal, M., Rivadulla, F., Saxena, S. S., Ahilan, K., & Rivas, J. (2009) Nature of the high-
264 pressure tricritical point in MnSi. *Physical Review B* 79, 060401.
265
- 266 Sipp, A., Bottinga, Y., and Richet, P. (2001) New high viscosity data for 3D network liquids and
267 new correlations between old parameters. *Journal of non-crystalline solids* 288,166-174.
268
- 269 Sonnevile, C., De Ligny, D., Mermet, A., Champagnon, B., Martinet, C., Henderson, G. H.,
270 Deschamps, T., Margueritat, J., and Barthel, E. (2013) In situ Brillouin study of sodium
271 alumino silicate glasses under pressure. *The Journal of Chemical Physics* 139, 074501.
272
- 273 Stebbins, J.F., and Sykes, D.(1990) The structure of $\text{NaAlSi}_3\text{O}_8$ liquid at high-pressure - New
274 constraints from NMR- spectroscopy. *American Mineralogist* 75, 943-946.
275
- 276 Stebbins, J. F., Wu, J., and Thompson, L. M. (2013) Interactions between network cation
277 coordination and non-bridging oxygen abundance in oxide glasses and melts: Insights from
278 NMR spectroscopy. *Chemical Geology* 346, 34-46.
279

- 280 Swainson, I. P., Tucker, M. G., Wilson, D. J., Winkler, B., & Milman, V. (2007). Pressure
281 response of an organic-inorganic perovskite: Methylammonium lead bromide. *Chemistry*
282 *of materials* 19, 2401-2405.
283
- 284 Walker, I. R. (1999) Nonmagnetic piston–cylinder pressure cell for use at 35 kbar and above.
285 *Review of scientific instruments* 70, 3402-3412.
286
- 287 Wang, X. F., Liu, R. H., Gui, Z., Xie, Y. L., Yan, Y. J., Ying, J. J., Luo, X.G. and Chen, X. H.
288 (2011). Superconductivity at 5 K in alkali-metal-doped phenanthrene. *Nature*
289 *communications* 2, 507.
290
- 291 Wu, J., Deubener, J., Stebbins, J.F., Grygarova, L., Behrens, H., Wondraczek, L., and Yue, Y.,
292 (2009) Structural response of a highly viscous aluminoborosilicate melt to isotropic and
293 anisotropic compression. *Journal of Chemical Physics* 131, 104504-1-10.
294
- 295 Xue, X., & Stebbins, J. F. (1993) ^{23}Na NMR chemical shifts and local Na coordination
296 environments in silicate crystals, melts and glasses. *Physics and Chemistry of Minerals*
297 20, 297-307.
298
- 299 Yarger, J. L., Smith, K. H., Nieman, R. A., Diefenbacher, J., Wolf, G. H., Poe, B. T., and
300 McMillan, P. F. (1995) Al coordination changes in high-pressure aluminosilicate liquids.
301 *Science* 270, 1964-1967.
302

303

304

Figure Captions

305

306

307

308

309

310

Figure 1. Pressure cell schematic. External pressure is applied to advance a piston and compress a PTFE cup containing a pressure transmitting fluid. A sample suspended in the fluid experiences hydrostatic pressure and a custom NMR coil placed around the sample allow for in-situ HP-NMR experiments. All component materials are chosen such that the pressurizing cell is completely non-magnetic. *Cell components shown are not to scale.

311

312

313

314

315

316

317

Figure 2. Static²³Na NMR spectra of albite glass collected *in situ* up to 2.0 GPa shown on a frequency scale relative to the peak position at 0 GPa. Spectra collected at 0, 1, and 2 GPa are shown as black lines labeled in order of increasing pressure from bottom to top with the spectrum collected after decompression to room pressure (red line) shown first in the sequence. Inset shows magnified view of the peak positions of spectra collected at 0 (black line), 0.5 (red line), 1.5 (blue line), and 2.0 GPa (green line). Spectra labeled in order of increasing pressure from bottom to top).

318

319

320

321

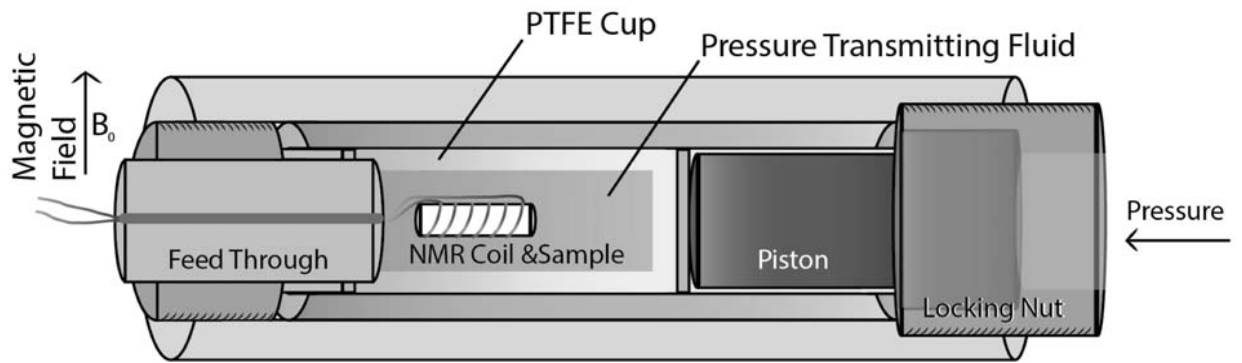
322

Figure 3. *Top*) Relative shift of the ²³Na NMR peak maximum (filled squares) and calculated average Na-O bond distance (open squares) for albite glass as a function of pressure. *Bottom*) Percent volume change calculated from reduction in the average Na-O distance only (filled circles-This study) and reported for bulk albite glass (open circles-Kuryaeva and Surkov, 2010) as a function of pressure.

323

324
325
326
327
328
329
330
331
332
333
334

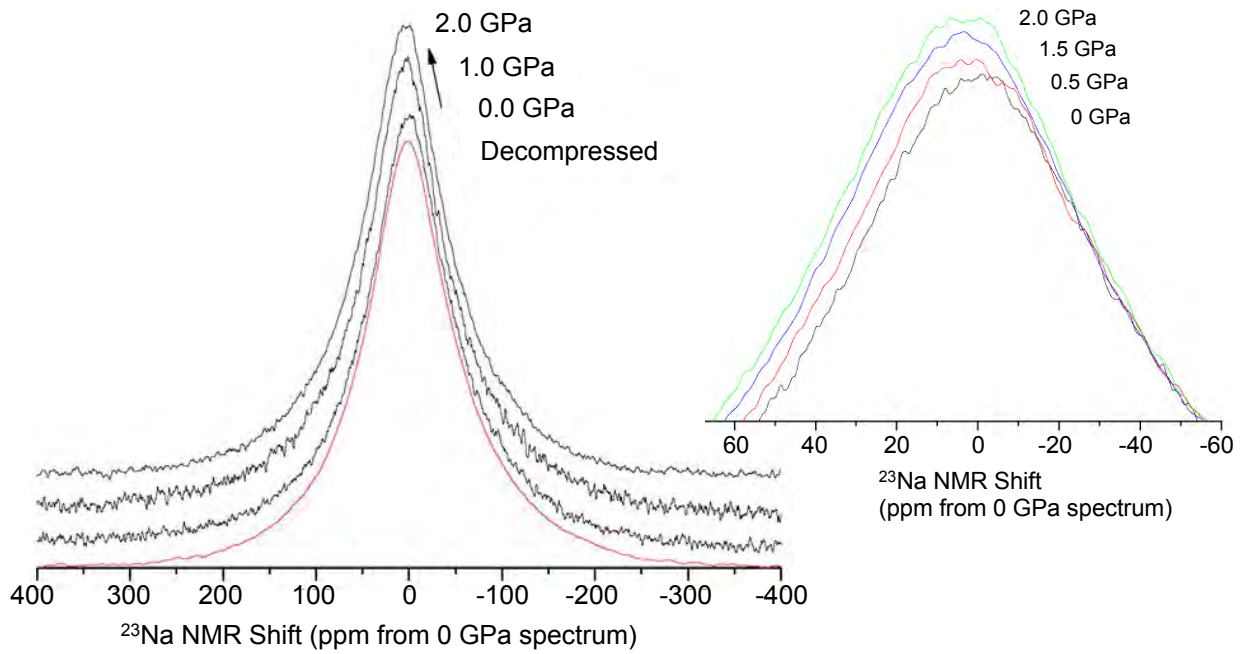
Figure 1



335
336

337
338
339
340

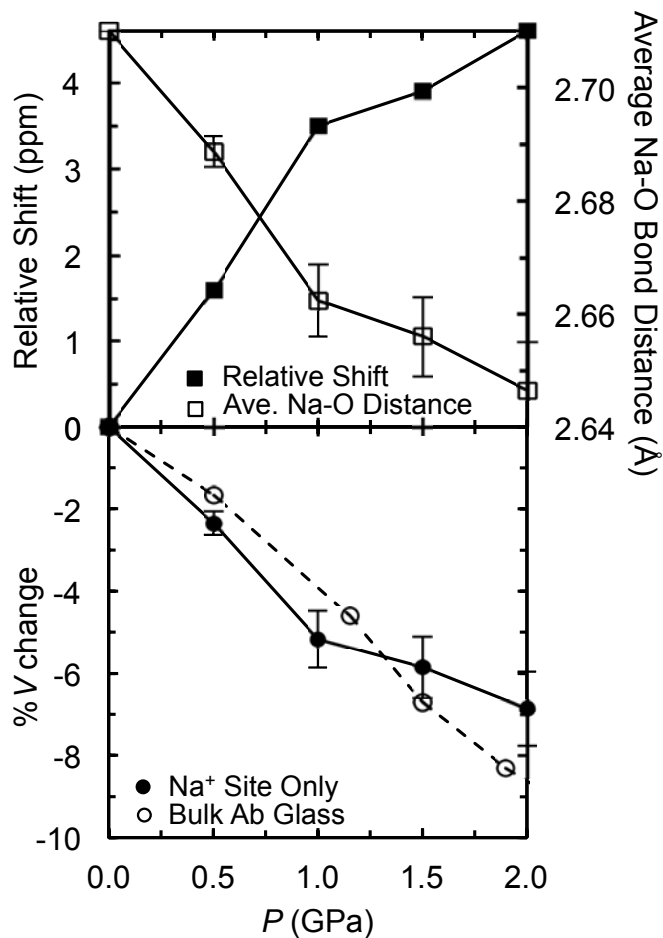
Figure 2



341
342
343
344

345
346
347
348
349
350

Figure 3 top and bottom



351
352

